

Mixed-1,10-phenanthroline with Mn(II), Cu(II), Co(II), Hg(II) and Ni(II) complexes Synthesis, Antimicrobial Activity and Spectroscopic Characterization of Binuclear Schiff Base

Rehab K. Al-Shemary¹, Eman Mutar Atiyah², Alaa Majid Sadiq³

Department of Chemistry, College of Education for Pure Sciences, Ibn -Al-Haitham, University of Baghdad

Abstract: A new series of mixed complexes were synthesized as $[Mn_2(phen)_2(L)]^{+2}$, $[Co(phen)_2(L)(H_2O)_2]^{+2}$, $[Ni_2(phen)_2(L)]^{+2}$, $[Cu_2(phen)_2(L)]^{+2}$ and $[Hg_2(phen)_2(L)(H_2O)_2]^{+2}$ by the template reaction between $H_2L = [2E,2'E)-2,2'-(biphenyl-4,4'-diylbis(azan-1-yl-1-ylidene))diacetic acid]$, phen = 1,10-phenanthroline; and $M(II) = Mn(II), Co(II), Cu(II), Ni(II)$ and $Hg(II)$ chloride salts. The structures of the compounds elucidated by IR, elemental analysis, and ^{13}C and 1H NMR (only ligand (H_2L)). The complexes have 1:2 electrolyte behavior in ethanol solution. The mixed complexes, their free ligands alongside the corresponding metal salts were screened against selected four bacterial isolates as (*Staphylococcus aureus*), (*Escherichia coli*), *Bacillus* and (*Pseudomonas*). All the mixed complexes showed enhanced antibacterial activities compared to their free ligands.

Keywords: Mixed complexes, binuclear, 1,10-phenanthroline, antibacterial activities

1. Introduction

Schiff bases with powerful donor atoms such as imine nitrogen and carboxylate oxygen are extraordinary in catalysis, structural richness and wide range of biological applications [1]. Binuclear Schiff base is coordinate very strong with transition metal ions [2] due to their usefulness in to understand the nature of exchange interactions operating between metals present in polymers, clusters and [3], effective devices [4] therefore they are very important in magneto-chemistry [5] and assembly of external species [6] and also find in medicine as chemotherapeutic agent [7], magnetic resonance imaging contrast agent [8], rheumatic drugs are Materials and Reagents: as antiviral, antifungal, antibacterial, and anticancer drugs [9]. Therefore, the topic of continuous investigation about functional and designing structural binuclear complexes [10].

The Schiff base complexes were derivative from nickel ions display obvious fungal activities [11], antibacterial activities [12], cytotoxic activity [13] and against human pathogenic bacteria [14]. Copper and Nickel complexes may be acted as therapeutic agents is notable and well established [15]. In this work Synthesized mixed binuclear Schiff base metal complexes with 1,10-phenanthroline and tetradentate ligand derived from benzidine as a result of big biological applications for ligand and its complexes [16].

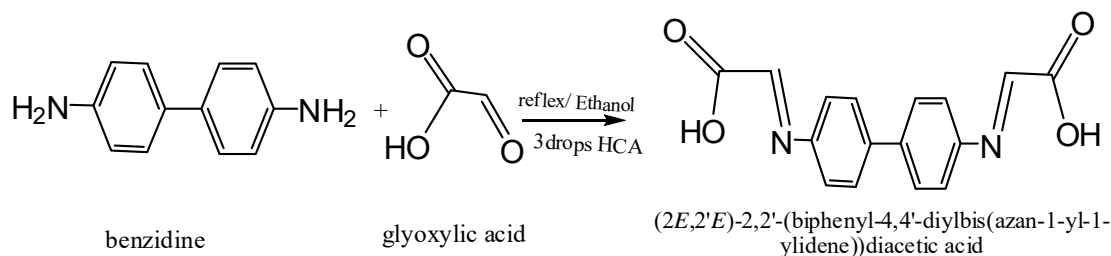
2. Measurements

The following measurements were used to characterize the ligand and its complexes. An electro thermal apparatus

Stuart melting points. Magnetic susceptibilities of the complexes were determined on Gouy balance model 7550 using. The diamagnetic corrections of the complexes were computed using Pascal's constants. FT-IR spectra were recorded by using Shimadzu, (FT-IR)-8300, Infrared Spectrophotometer in the range (4000-400) cm^{-1} . Spectra were recorded as potassium bromide discs. UV-Vis spectra of mixed -ligand complexes in DMSO were determined on Shimadzu UV-Vis 1601 spectrophotometer.

Preparation of binuclearing tetradentate Schiff base ligand [10]

The binuclearing tetradentate Schiff base was prepared by condensation of (gm, 2m mole) and glyoxylic acid (scheme 1n reaction in which (0.27gm, 2m mole) of glyoxylic acid dissolving in (10) ml of methanol was added to solution contain (0.06gm, 1mmole) of (0.27gm, 2m mole) dissolving in 10 ml of ethanol with continuous stirring, (three drops of Glacial acetic acid was added), After complete addition the reaction mixture was heated under reflux for about 4 hours. Then the volume of reaction mixture reduced was then by slow evaporation at room temperature. The recrystallizing for the product occurred by using hot ethanol, finally it was dried over anhydrous $CaCl_2$ in desiccators under reduced pressure.

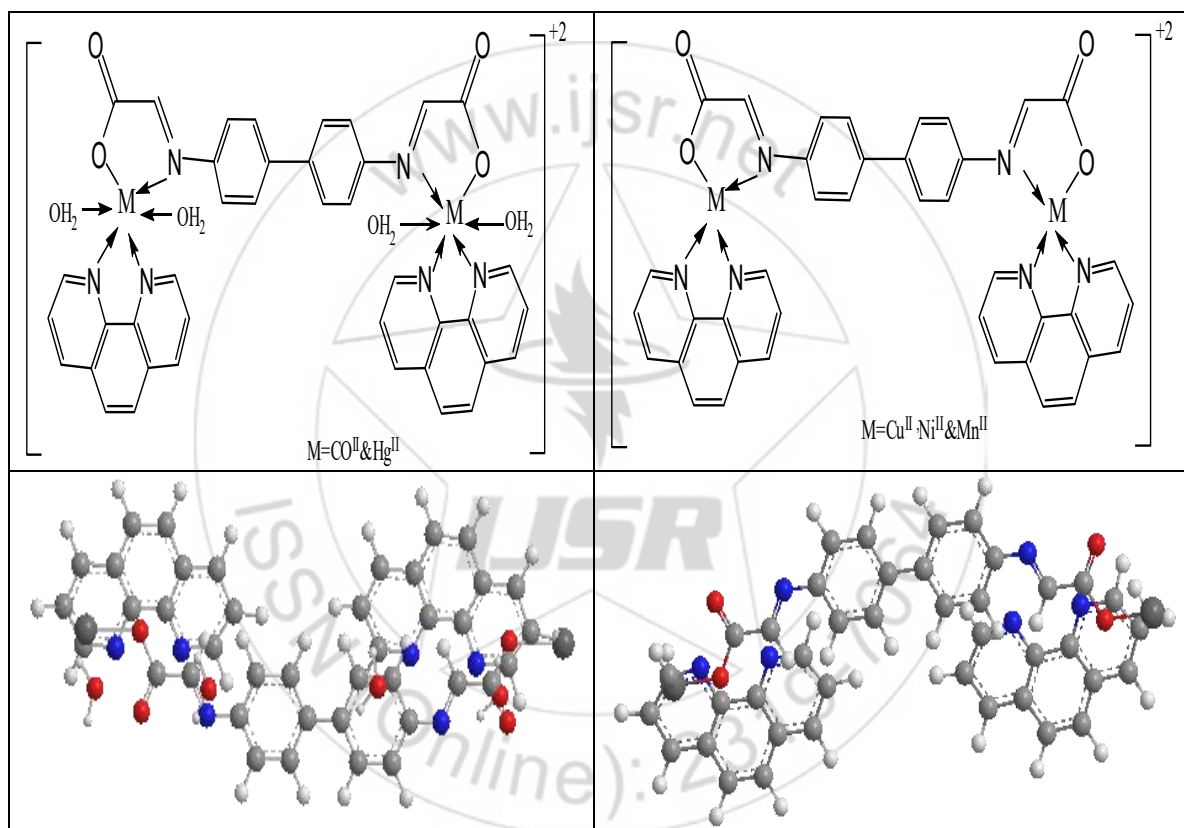


Scheme 1 Structure of binucleating tetradentate Schiff base ligand

Preparation of Metal Complexes

An aqueous solution of the metal salts containing (0.396g $\text{MnCl}_2 \cdot 4\text{H}_2\text{O}$, 0.476g $\text{CoCl}_2 \cdot 6\text{H}_2\text{O}$, 0.474g $\text{NiCl}_2 \cdot 6\text{H}_2\text{O}$, 0.21g $\text{CuCl}_2 \cdot 2\text{H}_2\text{O}$, and 0.542g HgCl_2) (2mmole) respectively with stirring and added gradually to ethanolic KOH solution (0.29g, 1mmole) of H_2L , an ethanolic solution

of (0.18g, 1mmole) 1,10-phenanthroline was added to the mixture in each case by using stichiometric amount (2:1:2) (Metal: ligand: phen) molar ratio. The mixture was refluxed with constant stirring for about 1~2 hours. The mixture was cooled at room temperature yellow precipitate was formed, filtered and recrystillized from methanol.



Scheme 2: Molecular structure of mixed ligand complexes

NMR spectrum for the ligand (H_2L)

$^1\text{H-NMR}$ spectrum of the ligand(H_2L) in DMSO-d_6 Table (2), Fig. (3) is characterized by the appearance of chemical shift related to The proton of the protons aromatic at (7.96-5.45)ppm. The characteristic signals at (8.06)ppm. is assigned to $\text{HC}=\text{N}$. The COOH signals is found at (9.98-10.86) ppm. The DMSO signal appeared at (2.50) ppm. [13].

$^{13}\text{C-NMR}$ of the free ligand (H_2L) Table (3) Fig(4) shows the $\text{HC}=\text{N}$ peak at (123.45) ppm., the COOH peak at (159.83) ppm, and carbon peaks for aromatic are detected at (112.5-118.41) ppm. the peak at (40.25) ppm. assigned to DMSO [14].

Electronic spectra, agnatic moments and conductivity measurements

The magnetic moment for some complexes are displayed in Table (5), The $\text{Ni}^{\text{(II)}}$ (1.86B.M.), $\text{Mn}^{\text{(II)}}$ (4.56B.M) and $\text{Cu}^{\text{(II)}}$ (1.98B.M) are consist with a tetrahedral geometry and $\text{Co}^{\text{(II)}}$ (5.42B.M) is octahedral geometry, [15].

The electronic spectrum of ligand (H_2L), Figure (3) exhibit high intense absorption peaks at (246 nm) (39062 cm^{-1}) and (334nm) (29940 cm^{-1}) which due to ($\pi \rightarrow \pi^*$) and ($n \rightarrow \pi^*$) transitions respectively, the data recorded in Table (5).

The electronic spectrum of 1,10-phenanthroline, Figure (4) displays high intense absorption bands at (202 nm) (49504

cm^{-1}) and (228 nm) (43859 cm^{-1}) which assigned to ($\pi \rightarrow \pi^*$) and band at (264 nm) (37878 cm^{-1}) which assigned to ($n \rightarrow \pi^*$) transition respectively, the data recorded in Table (5)[13]. These transitions were also found in the spectra of the complexes, but they were shifted towards lower in range ($30769\text{-}28571 \text{ cm}^{-1}$) [14].

The electronic spectrum of $[\text{Co}(\text{phen})_2(\text{L})(\text{H}_2\text{O})_2]^{+2}$ showed one intense peak in (261nm) (38314 cm^{-1}) was assigned to the ligand field. And another intense peak in (350nm) (28571 cm^{-1}) due charge transfer transition. And the peaks at visible region at (761 nm) (13140 cm^{-1}) and (832nm) (12019 cm^{-1}). These peaks are assigned to (${}^4\text{T}_{1\text{g}(\text{F})} \rightarrow {}^4\text{A}_{2\text{g}(\text{P})}$) and (${}^4\text{T}_{1\text{g}(\text{F})} \rightarrow {}^4\text{T}_{2\text{g}(\text{F})}$) (d-d) transitions confirming an octahedral structure around (Co^{+2}) ion complex [16].

The electronic spectrum of $[\text{Ni}_2(\text{phen})_2(\text{L})]^{+2}$ displayed one intense peak in (259nm) (35211 cm^{-1}) was assigned to the ligand field. And another intense peak in (355 nm) (28169 cm^{-1}) due charge transfer transition. And the peaks at visible region at (632 nm) (15822 cm^{-1}), (675nm) (14814 cm^{-1}) and (741nm) (13494 cm^{-1}). These peaks are assigned to (${}^3\text{T}_{1(\text{F})} \rightarrow {}^3\text{T}_{1(\text{P})}$), (${}^3\text{T}_{1(\text{F})} \rightarrow {}^3\text{A}_{2(\text{F})}$) and (${}^3\text{T}_{1(\text{F})} \rightarrow {}^3\text{T}_{2(\text{F})}$) (d-d) transitions confirming an tetrahedral structure around (Ni^{+2}) ion complex [17].

The electronic spectrum of $[[\text{Mn}_2(\text{phen})_2(\text{L})]^{+2}$ showed one intense peak in (276 nm) (36231 cm^{-1}) was assigned to the ligand field. And another intense peak in (365nm) (26041 cm^{-1}) due charge transfer transition. And the peak at visible region at (784nm) (12755 cm^{-1}). This peak was assigned to (${}^6\text{A}_{1(\text{P})} \rightarrow {}^4\text{E}_{(\text{G})}$) (d-d) transition confirming tetrahedral structure around (Mn^{+2}) ion complex [18].

The electronic spectrum of $[\text{Cu}_2(\text{phen})_2(\text{L})]^{+2}$ showed one intense peak in (331nm) (30211 cm^{-1}) due charge transfer transition. And the peak at visible region at (673nm) (14858 cm^{-1}). This peak was assigned to (${}^2\text{T}_2 \rightarrow {}^2\text{E}$) (d-d) transition confirming tetrahedral structure around (Cu^{+2}) ion complex [19].

The electronic spectrum of $[\text{Hg}_2(\text{phen})_2(\text{L})(\text{H}_2\text{O})_2]^{+2}$ showed absorption peak in (258 nm) (38759 cm^{-1}) was assigned to the ligand field. And another intense peaks in (351 nm) (28490 cm^{-1}) and (386nm) (25906 cm^{-1}) due charge transfer transition. The absence of absorption peaks at the visible region indicated no d-d electronic transitions happened, this is a good result for an octahedral structure around (Hg^{+2}) ion complex [20]. Where a comparison between the data recorded of the free ligand and mixed ligand complexes with Mn(II), Cu(II), Co(II), Ni(II) and Hg(II) metal ions are given in Table (5). The molar conductivities indicate that all metal complexes are 1:2 electrolytes Table (5). These data together with magnetic moment indicate tetrahedral geometry around the $\text{Mn}^{(\text{II})}$, $\text{Cu}^{(\text{II})}$ and $\text{Co}^{(\text{II})}$ metal atoms, and square planer geometry around $\text{Ni}^{(\text{II})}$, $\text{Hg}^{(\text{II})}$ metal atoms studied [21], Table (5).

3. Infrared studies

The FT-IR spectra assignment of the suggested structure of Schiff base complexes were formed through regard of their

infrared spectra. By the comparison method of FT-IR spectra of the free ligand and its mixed complexes from the coordinated stretching vibration peaks of products [22]. The above FT-IR data clearly indicate that the carbonyl groups of glyoxylic acid have reacted with the amine groups of benzidine through the condensation of the metal [23]. The FT-IR spectra of the Schiff base ligand displayed a sharp band at (1606 cm^{-1}) referred to $\nu(\text{C}=\text{N})$ azomethine group, the data was tabulated in (Table 3). The FT-IR spectra of the complexes which was shifted to lower frequency in range ($1602\text{-}1593 \text{ cm}^{-1}$), this is indicating the involvement of the coordination of imine nitrogen to the metal ion [24]. In the spectrum of the 1,10-phenanthroline appeared the band (1620) due to $\nu(\text{C}=\text{N})$ azomethine group. On complexation, this band was shifted to lower frequency in range ($1620\text{-}1618 \text{ cm}^{-1}$) for all the mixed complexes which suggest that the $\nu(\text{C}=\text{N})$ azomethine group is involved in coordination with 1, 10-phenanthroline compound. In the far IR spectra of the complexes, the non-ligand bands spotted at ($644\text{-}636 \text{ cm}^{-1}$) region assigned $\nu(\text{M-N})$ [25].

The disappearance $\nu(\text{OH})$ band of the Schiff base ligand in the spectra of the complexes indicating deprotonation of Schiff base ligand prior to coordination. But in the $[\text{Co}(\text{phen})_2(\text{L})(\text{H}_2\text{O})_2]^{+2}$ and $[\text{Hg}(\text{phen})_2(\text{L})(\text{H}_2\text{O})_2]^{+2}$ complexes appeared broad band at (3564 cm^{-1} and 3564 cm^{-1}), the weak bands at (925 cm^{-1}) and (968 cm^{-1}) were due to $\nu(\text{OH})$ and $\delta(\text{OH})$ for all the complexes refer to presence to coordinate aqua (H_2O) [26]. On the other hand, a considerable change in the position and intensity to lower wave number was observed on complexation with metal ion for the strong band in the Schiff base ligand spectrum at 1691 cm^{-1} , which appears due to $\nu(\text{COO})$ stretching vibration [27], these stretching vibrations are shifted to lower frequencies at ($1490\text{-}1482 \text{ cm}^{-1}$) and ($1326\text{-}1317 \text{ cm}^{-1}$) for all the complexes, ($\Delta\nu_{\text{asym.}} - \Delta\nu_{\text{sym.}}$) = ($161\text{-}171 \text{ cm}^{-1}$), supporting the idea that the ligand coordinate through deprotonated oxygen of carboxylate [28]. The broad bands at range ($3402\text{-}3444 \text{ cm}^{-1}$) and the weak bands at ($925\text{-}968 \text{ cm}^{-1}$) were due to $\nu(\text{OH})$ and $\delta(\text{OH})$ for all the complexes refer to presence to coordinate aqua (H_2O) [29]. Conclusive evidence regarding the bonding of oxygen to the metal ions is provided by the occurrence of bands at ($452\text{-}420 \text{ cm}^{-1}$). Accordingly, the ligand was bonded to the metal ion via two (COO^-) carboxylic oxygen atoms and two $\nu(\text{C}=\text{N})$ azomethine nitrogen atoms therefore the ligand is type of a tetradentate.

4. Antibacterial Activity Studies

Finally, the in vitro antibacterial activities of the ligand (H_2L) and their complexes were tested against (*Staphylococcus aureus*), (*Escherichia coli*), *Bacillus* and (*Pseudomonas*) using well diffusion method by nutrient agar as medium at (10^{-3}) mole/liter concentration was prepared by dissolving the compound in water. The zone of inhibition of bacterial evolution around the disc is offered in Fig 3. Table 4 displays the deactivation capacity versus the bacteria specimen of the synthesized compounds under work [31].

5. Conclusion

The N₂O₂ type Schiff base ligand is prepared from glyoxylic acid and benzidine. It acts tetradentate ligand and forms mixed complexes with transition ions such as Co^(II), Cu^(II), Ni^(II), Mn^(II), and Hg^(II). The ligand and its complexes are characterized using spectra and analytical data. All the mixed complexes have higher antimicrobial activity than the Schiff base ligand.

References

- [1] S. Khandar, A. Hosseini-Yazdi, and S. A. Zarei, "Synthesis, characterization and X-ray crystal structures of copper (II) and nickel (II) complexes with potentially hexadentate Schiff base ligands" *Inorganica Chimica Acta*, 358(11), pp.3211–3217, 2005.
- [2] D. P. Kessissoglou, M. L. Kirk, M. S. Lah et al., "Structural and magnetic characterization of trinuclear, mixed-valence of the ligand 1, 2-di [4-(2-imino 4-oxo pentane) phenyl] ethane" *Polyhedron*, 25(16), pp 3201–3208, 2006.
- [3] J.Sh. Sultan, F. H. Mosa, "Synthesis and Characterization of [2-(carboxy methylene-amino)-phenyl imino] acetic acid (L) and its some metal complexes" *J. Baghdad for Sci*, 10(3) 2013.
- [4] Z. H. Chohan, A. Munawar and C.T. Supuran, Transition metal ion complexes of Schiff's-bases synthesis; characterization and antibacterial properties Metal-based drugs, 8, pp. 137-143, 2001.
- [5] A. F. Cotton and G. S. Wilkenson, *Advanced inorganic chemistry*, 5th edition; John Wiley and Sons USA, pp.37-50, 1988
- [6] P.G. Cozzi, Metal–Salen Schiff base complexes in catalysis; Practical aspects. *Chem. Soc. Rev.*, 33, pp. 410-421, 2004.
- [7] M.A. Cusumano, M. Messina, F. Nicolo, M.L.D. Pietro, A. Rotondo, and E. Rotondo, NMR Study of L-Shaped Quinoxaline Platinum(II) Complexes- Crystal Structure of [Pt(DMeDPQ)(bipy)](PF₆)₂, *Eur.J. Inorg.Chem.*, 2004, pp.4710-4717.
- [8] Mei Wang, Hongjun Zhu, KunJin, Dong Dai and Licheng Sun., Ethylene oligomerization by salen-type zirconium complexes to low-carbon linear α -olefins.; *J.Catal.* 220, pp. 392-398, 2003.
- [9] N. Hirayama, I. Takeuchi, T. Honjo, K. Kubono and H. Kokusen, Ion-pair extraction system for the mutual separation of lanthanides using divalent quadridentate Schiff bases *Anal. Chem.*, 69, pp.4814-4818, 1997.
- [10] C.M. Metzler, A. Cahil and D. E. Metzler, "Equilibria and absorption spectra of Schiff bases,"; *J. Am. Chem. Soc.*, 102, pp. 6075-6082, 1980.
- [11] D.Chen and A.E.Martell, "Dioxygen affinities of synthetic cobalt Schiff base complexes," *Inorg. Chem.*, 26, pp. 1026-1030, 1987.
- [12] Loncle C, Brunel JM, Vidal N, Dherbomez M and Letourneux Y, "Synthesis and antifungal activity of cholesterol-hydrazone derivatives", *Eur. J. Med. Chem.*, 39, 1067-1071, 2004.
- [13] S. Papakonstantinou-Garoufalias, N. Pouli, P. Marakos and A. Chytyroglou-Ladas, "Synthesis antimicrobial and antifungal activity of some new 3 substituted derivatives of 4-(2, 4-dichlorophenyl)-5-adamantyl-1H-1, 2, 4-triazole", *Farmaco*, 57, pp. 973-977, 2002.
- [14] B. K. Kaymakcioglu and S. Rollas, "Synthesis, characterization and evaluation of antibuberculos activity of some hydrazones", *Farmaco*, 57, pp. 595-599, 2002.
- [15] R. Maccari, R. Ottana and M.G. Vigorita, "In vitro advanced antimycobacterial screening of gonifoniazid-related hydrazones, hydrazides and cyanoboranes: Part 14", *Bioorg. Med. Chem. Lett.*, 15, pp. 2509-2513, 2005.
- [16] M. T. Cocco, C. Congiu, V. Onnis, M. C. Pusceddu, M. L. Schivo and A. De Logu, "Synthesis and antimycobacterial activity of some isonicotinoyl hydrazones", *Eur. J. Med. Chem.*, 1076-1071, 34. 1999,
- [17] R. Vafazadeh and M. Kashfi, Synthesis and characterization of cobalt (II) octahedral complexes with flexible salpn Schiff base in solution. Structural dependence of the complexes on the nature of Schiff base and axial ligands; *Bull. Korean Chem. Soc.* 86: 697.28(7): 1227, 2007.
- [18] H. Hassib and A.A. Razik, Dielectric properties and A.C. conduction mechanism for 5,7-dihydroxy-6- formyl-2-methylbenzo-pyran-4-one bis-Schiff base; *Solid State Communication*, pp.147: 345, 2008.
- [19] S. Sarkar, V. Aydogdu, F. Dandelion, B.B. Bhaumik and K. Dey, X-ray diffraction studies, thermal, electrical and optical properties of oxovanadium (IV) complexes with quadridentate Schiff bases; *Material Chem. Phys.*, 88: 357, 2004.
- [20] M.A. Neelakantan, T. Jeyakumar, K. Muthukumar, Spectral, XRD, SEM and biological activities of transition metal complexes of polydentate ligands containing thiazole moiety; *Spectrochimica Acta Part A*, 71: 628, 2008.
- [21] A. A. Ahmed and S. A. BenGuzzi, Synthesis and Characterization of Some Transition Metals Complexes of Schiff Base Derived From Benzidine and Acetylacetone, *J. of Sci. and Appl.*, 2(1)83-90, 2008.
- [22] D. Chatterjee, A. Mitra and B.C. Roy, Oxidation of organic substrates catalyzed by a novel mixed-ligand ruthenium (III) complex. *J. Mol. Cat.*, 17, 161, 2000.
- [23] L. Singh, G. Mohan, R.K. Parashar, S.P. Tripathi and R.C. Sharma Studies on anti-inflammatory activity of some lanthanone complexes of bioactive organic molecules. *Curr. Sci.*, 55, 846, 1995.
- [24] A. Oswole., Syntheses and Characterization of Some Tetradentate Schiff-Base Complexes and Their Heteroleptic Analogues. *E-Journal of Chemistry*, 5(1) 130-135, 2008.
- [25] D.G. Rando, D.N. Sato, L. Siqueira, A. Malvezzi, C.Q.F. Leite, A.T. de Amaral, D. Shingnapurkar, S. Padhye and C. Ratledge, "Schiff base conjugates of p-aminosalicylic acid as antimycobacterial agents", *Bioorg. Med. Chem. Lett.*, 16, 1514-1517, 2006.
- [26] D.P. Singh, R. Kumar, R. Mehani and S.K. Verma, Synthesis and characterization of divalent metal complexes with ligand derived from the reaction of 4-aminopyridine and biacetyl. *J. Serb Chem Soc.*, 71, 939, 2006.
- [27] K. Deepa, N.T. Madhu, P.K. Radhakrishnan, Metal complexes of Schiff bases derived from dicinnamoyl

- methane and aromatic amines, *Synth. React. Inorg. Met. Org. Chem.* 35: 883, 2005.
- [28] R. Karvembu and K. Natarajan Synthesis and spectral studies of binuclear ruthenium(II) carbonyl complexes containing bis(β -diketone) and their applications, *Polyhedron*, 21, 219, 2002.
- [29] Ali SA, Soliman AA, Aboaly MM, Ramadan RM. Chromium, Molybdenum and Ruthenium Complexes of 2-Hydroxyacetophenone Schiff Bases. *J Coord Chem.* 55: 1161, 2002.
- [30] R. M. Silverstein, F.X. Webster and D. J. Kiemle, Spectrometric identification of organic compounds, John Wiley & Sons, 2005.
- [31] N. Mahalakshmi and R. Rajavel, Synthesis, Spectroscopic Characterization, DNA Cleavage and Antimicrobial Activity of Binuclear Copper (II), Nickel (II) and Oxovanadium(IV) Schiff Base Complexes, *Asian J. of Bio. And Pharm. Res.*, 2 (1), 525- 543, 2011.

Table 1: Several of physical properties of prepared ligand (H_2L) and its mixed complexes

Compounds	Empirical Formula	Molecular Weight	Yield %	M.P $^{\circ}$ C	Colour	% (Calc.) Found			
						C	H	N	Metal
H_2L	$C_{14}H_{16}N_2O_4$	296.28	81	171	Dark brown	(64.86) 63.67	(4.08) 4.40	(9.46) 9.21	-
$[Co_2(phen)_2(L)(H_2O)_2]^{+2}$	$C_{40}H_{34}Co_2N_6O_8$	844.60	76	232	Dark yellow	(56.88) 57.20	(4.06) 4.50	(9.95) 77.50	(13.96) 11.20
$[Ni_2(phen)_2(L)]^{+2}$	$[C_{40}H_{26}N_6Ni_2O_4]$	772.06	68	267	Greenish yellow	(62.23) 62.64	(3.39) 3.21	(10.89) 10.60	(15.20) 14.30
$[Mn_2(phen)_2(L)]^{+2}$	$C_{40}H_{26}Mn_2N_6O_4$	764.55	70	261	Pale brown	(62.84) 62.78	(3.43) 3.47	(10.99) 10.74	(14.37) 14.35
$[Cu_2(phen)_2(L)]^{+2}$	$C_{40}H_{26}Cu_2N_6O_4$	781.76	84	208	brown	(61.45) 61.69	(3.35) 3.32	(10.75) 10.56	(16.26) 15.80
$[Hg_2(phen)_2(L)(H_2O)_2]^{+2}$	$C_{40}H_{34}Hg_2N_6O_8$	1127.91	73	215	brown	(42.59) 41.89	(3.39) 3.47	(10.89) 10.69	(15.20) 14.64

Table 2: 1H -NMR Chemical shifts for Ligand (H_2L) (ppm in DMSO)

C-H _{aromatic}	HC=N	COOH
123.28-136.56	147.26	162.87

Table 3: ^{13}C -NMR Chemical shifts for Ligand (H_2L) (ppm in DMSO)

HC=N	C-H _{aromatic}	COOH
3.87	5.85-8.35	10.86

Table (4): Infrared spectral data (wave number ν') cm^{-1} for the ligand (H_2L), and its complexes

Compounds	ν_{OH}	$\nu_{C-H_{arom}}$	$\nu_{C-H_{aliph}}$	$\nu_{C=O}$	$\nu_{(C=N)imine}$	$\nu_{assm. C-OO^-}$	$\nu_{sym. C-OO}$	$\Delta\nu_{cm^{-1}}$	$\delta_{OH_{free}}$	M-N M-O
H_2L	3352	3053	2998	1678	1606	-	-	-	-	-
1,10-phenanthroline	-	3034	-	-	1620	-	-	-	-	-
$[Co_2(phen)_2(L)(H_2O)_2]^{+2}$	3564	3049	2937	-	1616 1600	1482	1320	162	842	640 452
$[Ni_2(phen)_2(L)]^{+2}$	-	3055	2991	-	1618 1600	1487	1326	161	-	644 420
$[Mn_2(phen)_2(L)]^{+2}$	-	3072	2987	-	1614 1602	1490	1322	168	-	636 428
$[Cu_2(phen)_2(L)]^{+2}$	-	3064	2999	-	1612 1598	1496	1325	171	-	644 448
$[Hg_2(phen)_2(L)(H_2O)_2]^{+2}$	3562	3049	2937	-	1611 1593	1486	1317	169	846	638 442

Table 5: Electronic spectral data of the ligand (H₂L) and its mixed complexes

Compound	μ_{eff}	$\frac{\Lambda_m}{2}$ S.Cm molar ⁻¹	λ_{nm}	ν -wave number cm^{-1}	Assignments	
H ₂ L	-	-	246	39062	$\pi \rightarrow \pi^*$	-
			334	29940	$n \rightarrow \pi^*$	
1,10-phenanthroline	-	-	202	49504	$\pi \rightarrow \pi^*$	-
			228	43859	$\pi \rightarrow \pi^*$	
			264	37878	$n \rightarrow \pi^*$	
[Co ₂ (phen) ₂ (L)(H ₂ O) ₂] ⁺	5.42	76	261	38314	L.F	Octahedral
			350	28571	C.T	
			761	13140	${}^4T_{1g(F)} \rightarrow {}^4A_{2g(P)}$	
			832	12019	${}^4T_{1g(F)} \rightarrow {}^4T_{2g(F)}$	
[Ni ₂ (phen) ₂ (L)] ⁺²	1.86	73	259	35211	L.F	Tetrahedral
			355	28169	C.T	
			632	14814	${}^3T_{1(F)} \rightarrow {}^3T_{1(P)}$	
			675	15822	${}^3T_{1(F)} \rightarrow {}^3A_{2(F)}$	
			741	13494	${}^3T_{1(F)} \rightarrow {}^3T_{2(F)}$	
[Mn ₂ (phen) ₂ (L)] ⁺²	4.56	75	276	36231	L.F	Tetrahedral
			365	26041	C.T	
			784	12755	${}^6A_{1(P)} \rightarrow {}^4E_{(G)}$	
[Cu ₂ (phen) ₂ (L)] ⁺²	1.98	77	331	30211	C.T	Tetrahedral
			673	14858	${}^2T_2 \rightarrow {}^2E$	
[Hg ₂ (phen) ₂ (L)(H ₂ O) ₂] ⁺	Dia	79	258	38759	L.F	Octahedral
			351	28490	C.T	
			386	25906	C.T	

Table 6: Diameter of zone of inhibition (mm)

Comp.	<i>Escherichia. Coli</i>	<i>Staphylococcus aureus</i>	<i>Bacillus</i>	<i>pseudomonas</i>
H ₂ L	-	1	4	2
[Co ₂ (phen) ₂ (L)(H ₂ O) ₂] ⁺²	3	7	10	13
[Ni ₂ (phen) ₂ (L)] ⁺²	5	8	11	9
[Mn ₂ (phen) ₂ (L)] ⁺²	9	12	9	12
[Cu ₂ (phen) ₂ (L)] ⁺²	6	10	6	8
[Hg ₂ (phen) ₂ (L)(H ₂ O) ₂] ⁺²	7	8	12	10

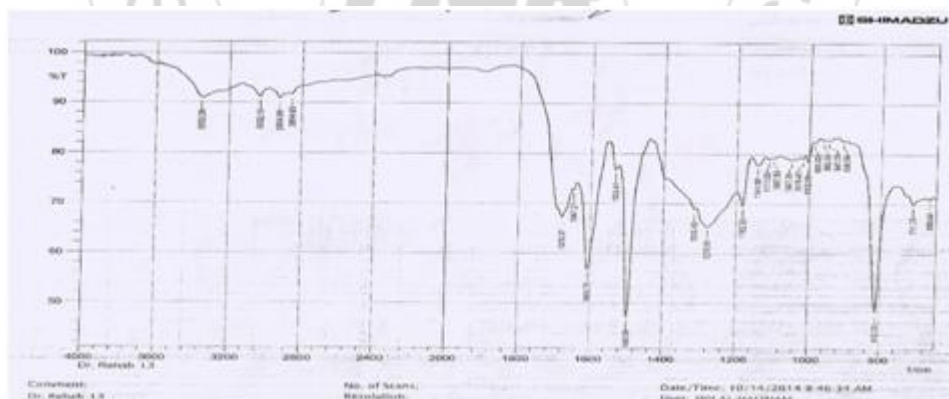


Figure 1: The IR spectrum of the ligand H₂L

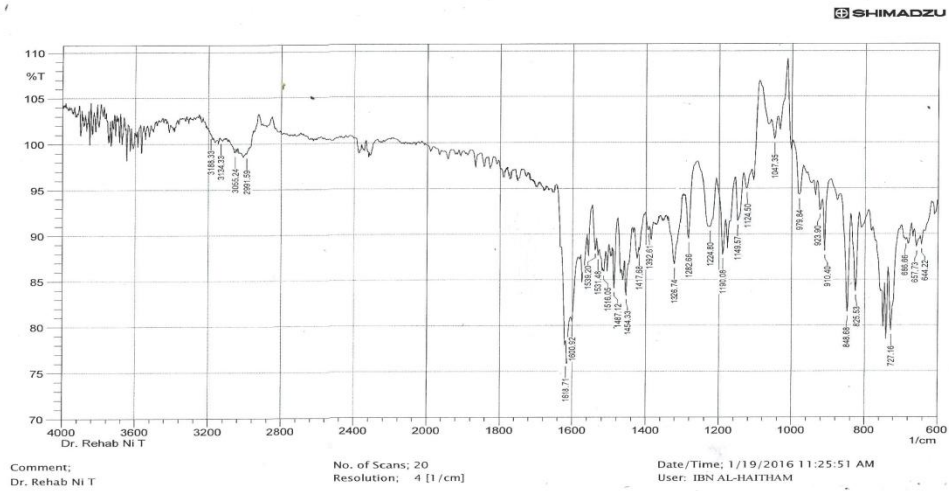


Figure 2: The IR spectrum of the $[Ni(phen)(L)]^{+2}$ complex

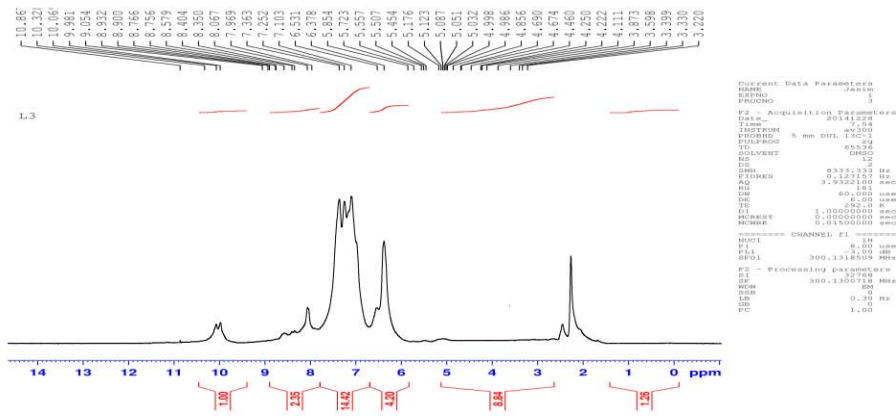


Figure 3: The 1H -NMR spectrum of the ligand (H_2L)

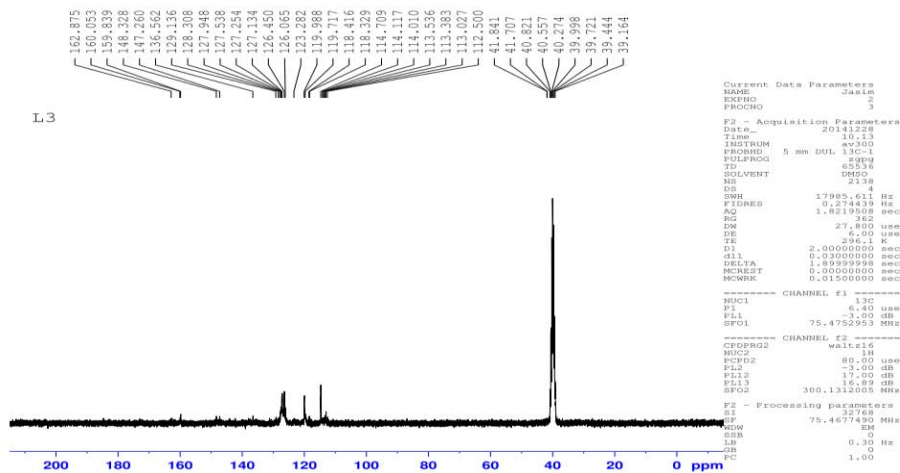


Figure 4: The ^{13}C -NMR spectrum of the ligand (H_2L)

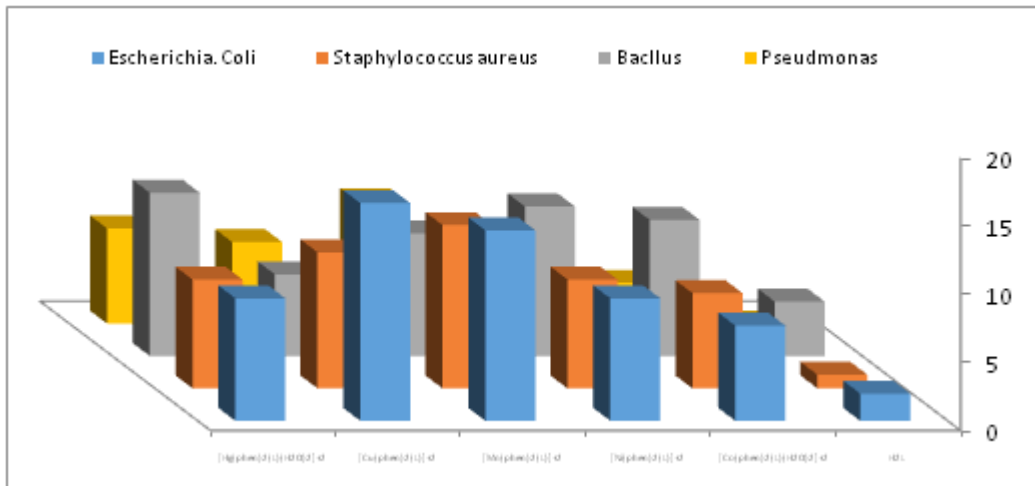


Figure 5: Difference between the antimicrobial activity of ligand(H₂L)& mixed complexes

